Design Considerations and Measured Performance of Nontracked Mirror-Augmented Photovoltaics

Wei-Chun Lin, *Student Member, IEEE*, Timothy J. Peshek, *Member, IEEE*, Laura S. Bruckman, Mark A. Schuetz, *Member, IEEE*, and Roger H. French, *Member, IEEE*

***Abstract*—Costs associated with conventional photovoltaic (PV) installations (module manufacturing, mounts, wiring and installation labor, etc.) scale linearly with system area, and prudent design practices for increasing the light harvesting may significantly enhance the power output per unit area and cost per watt. The use of PV modules that have been augmented by the addition of a solar mirror provides an opportunity to improve light harvesting of a PV module and cost-per-watt considerations if the mirror is less expensive than the relative increase in power. In order to harvest greater insolation, an optimized design configuration between a flat-panel module and mirror is necessary for a fixed (nontracked) mirror-augmented photovoltaic (MAPV) system. A series of irradiance and energy harvest calculations were developed to screen various MAPV design configurations. We employed optical ray-tracing simulations to determine irradiance nonuniformities on the fixed MAPV system. The simulated results are compared with outdoor experimental field trial results. Over a three-month period of study, the fixed MAPV system produced 12% more power than an equivalent nonaugmented panel. An adjustable angle mounting system known as "time machine" was used to estimate yearly power production by adjusting the relative position of the MAPV system to represent varying times of the year. Current–voltage (*I–V*) curve tracing of test modules was performed during the field trials on augmented and nonaugmented modules for comparison. The experimental time machine result is in agreement with the irradiance simulation, which shows a gullwing curve of annual power output with peak production on the equinoxes and reduced production on the solstices.**

***Index Terms*—Low concentration, mirror augmentation, photovoltaic (PV) systems, simulation.**

I. Introduction

THE large reduction of commercial photovoltaic (PV) pricing over the last few years has allowed favorable economics for multicrystalline silicon solar cells while reducing the competitiveness of other forms of PV, including thin-film technologies that employ concentration. Those technologies, including III–V multijunction cells, most commonly rely on dual-axis trackers and high-concentration systems to aid their cost/watt ratios. Concentrating photovoltaics (CPV) can provide benefits in the form of reduced balance-of-systems (BOS) costs. More power can be reaped from a cell, and less relative cost is required in the form of interconnects, inverters, racking, and real estate for CPV in comparison with conventional PV. We describe a system in which cost-effective solar mirrors are utilized with conventional polycrystalline Si (pc-Si) modules to augment the power production of these modules [1], [2]. This system takes advantage of the favorable cost structure of both the low cost of silicon modules as well as BOS benefits of CPV. An example of a commercial MAPV system supplier is TenK Solar, which provides modules paired with mirrors designed for enhanced light capture and, thus, increased power. In this scenario, the mirrors provide a low-concentration value, and this is referred to as mirror-augmented PV, (MAPV) [3]–[5].

Using solar mirrors to harvest more of the direct sunlight on qualified PV modules increases the electricity produced from a given area of PV panels [3]. Replex plastics has developed a high performance, low-cost solar back surface mirror made of acrylic. The acrylic mirror uses a back surface aluminum reflector and is ideal for PV augmentation because of its low cost, light weight, and low light scattering [2]. The back surface solar mirror can spectrally filter ultraviolet (UV) light, which prevents the PV panel from experiencing additional harmful UV irradiance reflected from the mirror [6]. We have also studied the lifetime and durability of the solar mirrors in previous studies [7], [8]. Therefore, MAPV systems can improve the harvesting of the fixed 1 kW/m^2 solar resource, and may not include a lifetime performance penalty due to more rapid PV module degradation.

The MAPV system still has challenges that need to be solved. Among these challenges is maximizing energy harvest when the angle of insolation is constantly changing. The most straightforward solution is to place PV modules and mirrors on a solar tracker, ensuring a near-constant incidence angle of illumination [9]. Although a tracked MAPV system can harvest more light, the cost is also increased greatly [10]. A fixed MAPV system offers a low-cost solution, but introduces irradiance nonuniformity issues upon the module [2], [4]. The challenge of fixed MAPV is in optimizing the system properly to maximize the annual power production for a system, where the irradiance and thermal variations are complex [5]. The cell string architecture of a standard pc-Si PV module is not ideal for MAPV due to the inherently nonuniform irradiance [11]. The current matching of cells in a commercial module demand that the irradiance be uniform, but this restriction can be mitigated through the use of submodular dc/dc microconverters to perform, for example,

Manuscript received September 30, 2014; revised January 22, 2015; accepted February 3, 2015. Date of publication April 8, 2015; date of current version April 17, 2015. This work was supported by Ohio Third Frontier under Tech 11-060 and Tech 12-004, as well as by the Clinical and Translational Science Award 1 UL1 RR024989 from NCRR/NI for the REDCap sample management database.

W.-C. Lin, T. J. Peshek, L. S. Bruckman, and R. H. French are with the Solar Durability and Lifetime Extension Center, Department of Materials Science and Engineering, Case Western Reserve University, Cleveland, OH 44106 USA (e-mail: wxl157@case.edu; tjp3@case.edu; lsh41@case.edu; rxf131@case.edu).

M. A. Schuetz is with Replex Plastics, Mount Vernon, OH 43050 USA (e-mail: mark@replex.com).

Color versions of one or more of the figures in this paper are available online at http://ieeexplore.ieee.org.

Digital Object Identifier 10.1109/JPHOTOV.2015.2405758

substring power conversion and maximum power point tracking [12] for modules in landscape orientation. Hence, the goals for fixed MAPV with pc-Si PV modules are to obtain the most uniform irradiance distribution possible while producing maximum annual energy harvest as well.

II. Simulation Methods and Tools

A. One-Dimensional Geometrical Irradiance Model Development

As a proof-of-concept model, the performance of the mirror-augmented system is calculated analytically in MATLAB by considering only one dimension and no material features of the reflector. The module and mirror configuration are assumed to be infinite in length and hold translational symmetry. Additionally in this proof-of-concept model, no cloud cover or weather is considered. Our objectives were to demonstrate the improvement in average annual power production for an MAPV module in comparison with a nonaugmented module, and to model the design elements of the mirror, such as optimal tilt angle and mirror throw distance. To meet these objectives, we varied the solar position for every minute for the given installation location based on a technical report developed by Reda and Andreas in NREL [13]. Detailed information on the solar position relative to longitude and latitude coordinates were used to determine the incidence angle of solar irradiance. For this case study, we selected the latitude and longitude of Columbus, OH, USA, because of access to experimental data for comparison, as described below. Total annual production is the time-integrated incident power upon the module from January 1 to December 31.

The air mass is the path length that light takes through the atmosphere normalized to the shortest possible path length. The air mass quantifies the reduction in the power of light as it passes through the atmosphere and is absorbed by air and dust. The theoretical air mass incorporates the curvature of the earth, as given by [14]

$$\mathrm{AM} = \frac{1}{\cos(\alpha_{\mathrm{sun}}) + 0.50572(96.07995 - \alpha_{\mathrm{sun}})} \tag{1}$$

where α_{sun} is the solar zenith angle (or 90°-solar elevation angle). The intensity of the direct component of sunlight throughout each day (I_{direct}) can be determined as a function of air mass from an empirical relation [15]

$$I_{\mathrm{direct}} = 1.353(0.7^{\mathrm{AM}^{0.678}}). \tag{2}$$

The global irradiance (I_{global}) normal to a module's surface is $1.1I_{\mathrm{direct}}$, due to the approximate 10% increase in irradiance from diffuse light, and represents the maximum possible irradiance. For a module surface that is nonnormal to the solar irradiance, (3) gives the dependence of insolation upon a rectangular surface S_m for arbitrary solar elevation angle and tilt angle

$$\begin{aligned} S_m = \; & I_G(\cos(\theta_{\mathrm{sun}})\sin(\theta_m)\cos(\phi_m - \phi_{\mathrm{sun}}) \\ & + \sin(\theta_{\mathrm{sun}})\cos(\theta_m)) \end{aligned} \tag{3}$$

where θ_{sun} is the solar elevation angle, ϕ_{sun} is the solar azimuth angle, θ_m is the module or mirror tilt angle, and ϕ_m is the azimuth angle of the module or mirror.

We calculated the mirror throw distance D_{mirror} using (4), shown below, which was obtained from geometric optics

$$D_{\mathrm{mirror}} = \frac{L_{\mathrm{mirror}}\sin(\theta_{\mathrm{sun}} - \theta_{\mathrm{mirror}})}{\sin(\theta_{\mathrm{panel}} - \theta_{\mathrm{sun}} + 2\theta_{\mathrm{mirror}})}. \tag{4}$$

The mirror throw distance represents the relative length of the augmentation region on a module to its total length in 1-D. The length of the mirror L_{mirror} was selected considering the module row packing density, and was set equal to the length of the module. This length may not be optimal for the system as will be shown in this paper. With changing solar incidence angles, it is evident that the throw distance will result in bands of irradiance augmentation on the module throughout most times. By adding the light intensities of PV panel and reflective mirror, the total amount of power generated by fixed MAPV can be obtained.

The annual power production was calculated for mirror tilt angles varying from 5° to 25°, in steps of 5°, as a function module tilt angle. The effects of the irradiance augmentation bands and their uniformity were explored using 3-D optical ray-tracing modeling, as described next.

B. Three-Dimensional Irradiance Ray-Tracing Model Development

In addition to the 1-D geometric irradiance model, we generated a full 3-D ray-tracing model of irradiance to optimize the MAPV system design, including nonuniformity terms. The irradiance nonuniformity is an important element in the study of the power production efficacy and estimate power degradation rates. PV modules that receive highly localized irradiance may experience faster module degradation rates due to the excess current loss as determined by string matching with less illuminated cells. Therefore, we employ ray tracing to simulate the light distribution on solar panel as a function of time of day and year [16].

Several ray-tracing software packages have been used in the literature to evaluate concentrated PVs, such as FRED [17], Apilux [18], ZEMAX [19]–[21], and TracePro.

Here we employ TracePro, developed by Lambda Research Corporation, to generate the 3+D irradiance results described in this paper. This software package allowed us to generate detailed ray-trace analysis on a model without making any assumptions as to the order in which objects and surfaces will be intersected. At each intersection, individual rays can be subject to absorption, reflection, refraction, diffraction, and scatter. Hence, a model of specific material properties at interfaces can be constructed in TracePro for physically relevant results using the properties of the acrylic back surface reflector mirrors. Furthermore, TracePro can construct 3-D solid models geometrically, and it is also compatible with other computer-aided design (CAD) programs such as SolidWorks.

Our procedure for optimizing the MAPV design involved importing models into TracePro and defining material and surface properties, such as reflection and absorption, for the appropriate

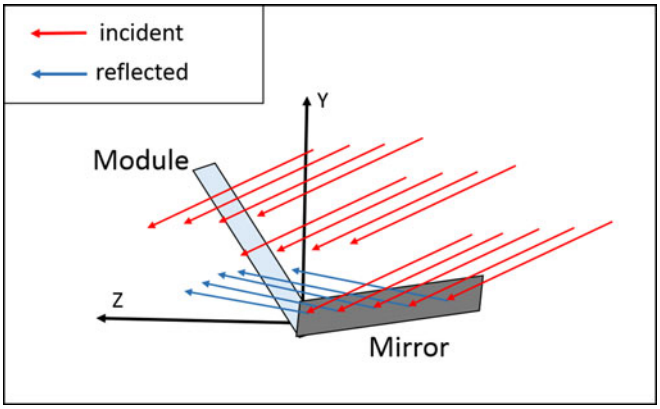

Fig. 1. Sketch of a TracePro 3-D model of a module and mirror system on January 15, with a small subset of the incident solar rays in red and reflected rays in blue.

objects in the model. The next step is the ray-tracing process in which the rays are traced from a solar light source onto the defined model. The final step is to analyze the ray-trace results to determine the location, extent, and distribution of the resultant illumination on the panel and mirrors.

Because of the computationally intensive 3-D model generation, we will limit the 3-D simulations presented here to the optimal results determined by the 1-D modeling. Our initial prototype model is a mirror of the same length as a module. Fig. 1 depicts a 3-D model of the module and mirror designed in CAD with solar rays incident upon the system.

C. Experimental Confirmation From Field-Test I–V Curve Tracing

An outdoor test facility was constructed at Replex Plastics (Mt. Vernon, OH, USA) for real-world data collection. Three PV panels (Canadian Solar CSI CS-6P 200W) were coupled with Replex back surface acrylic solar mirrors. A second row of three nonaugmented modules was also installed to enable simultaneous side-by-side comparison between mirror-augmented and nonaugmented modules. The mirror-augmented module was installed at the 1-D result-optimized 55° tilt angle, and two nonaugmented modules were installed at 1-D result-optimized 34° for a module with no mirror, and 55° for direct comparison with the MAPV system. An adjustable PV module mounting system (the 'time machine," as shown in Fig. 2.) was used to experimentally probe the relative position between the sun and the fixed MAPV system by appropriately tilting the module and mirror angle to achieve the correct relative positioning. This tilting of the time machine racking is allowed for an equivalent solar zenith angle to any time throughout the calendar year. The angles between the augmented modules and the mirrors were fixed on the time machine. Using knowledge of the current solar position, the time machine system was adjusted to simulate a different sun position and a different time of year. Hence, the integrated power output for an entire year was obtained in a short time.

A Daystar multitracer was used to load the modules and perform periodic *I–V* scans. The multitracer is a self-contained load and data acquisition device for collecting PV module

Fig. 2. Replex "time machine": A rotating tilt module/mirror combination that simulates different times of the year by varying the incident angle of the solar irradiance.

performance, while also collecting data from auxiliary sources that acquire irradiance and temperature data. *I–V* curves were then normalized to standard test conditions: 25 °C and 1000 W/m^2. Contact thermocouples (T-type) and a solar pyranometers (Kipp-Zonen CHP6) were obtained and calibrated for this purpose.

Results of the simulations were compared with the measured power produced for augmented, optimized modules, as well as nonaugmented modules at the same site for a period of time from January 6 to March 31.

Further the annual production measurements collected using the time machine were compared with simulation, and used to refine further iterations of models to optimize performance, whose results are presented in Section III.

III. Results and Discussion

A. Optimal One-Dimensional Mirror/Module Configuration for Annual Irradiance

The 1-D model generated in MATLAB was used to estimate the illumination pattern on a mirror-augmented module and to optimize the mirror and module configuration for maximized annual power output in Mount Vernon, OH, USA. We found that the system receives maximum irradiance for a module tilt angle $= 55°$, and mirror tilt angle $= 10°$, from the horizontal. Additionally, the calculations indicate that the optimal tilt angle for a nonaugmented module is 35°. If all of the augmented irradiance could be captured by the module, the maximum estimated annual energy harvest would increase by 12% over the nonaugmented counterpart mounted at its optimal tilt angle.

B. Three-Dimensional Optical Analysis and Nonuniformities

A CAD model of a module and mirror was designed and used as an initial model in TracePro. The models are oriented so that the z-direction is along the earth's North–South axis,

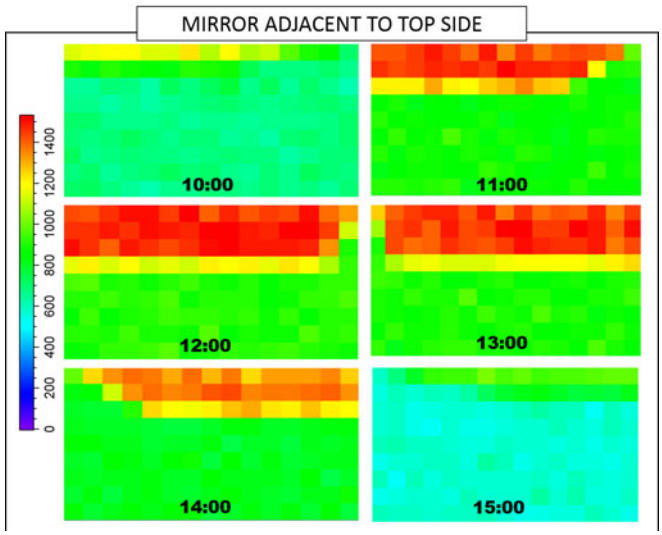

Fig. 3. Irradiance maps across the length and width of a 60-cell Si module, as determined by TracePro. The maps depict the augmentation strength and uniformity near noon time on an hourly basis. It was observed that the nonuniformity created intensity bands across the module length. The mirror adjoins the module at the top of the images.

the x-direction is along the East–West axis, and the y-direction is normal to the surface of the earth. The PV module and the mirror are positioned at the optimal tilt angles according to the results from the 1-D simulation.

In Fig. 3, we show the TracePro-generated incident irradiance upon the PV module at various times on March 15. These simulated results quantify the extent of time-dependent mirror augmentation nonuniformity. Nonuniformities arise from the variation in material properties, i.e., the contribution to absorption and scattering in the acrylic mirror and the insolation angle. The nonuniformity of augmentation can be positively affected by increasing the mirror length beyond what was simulated here. Naively, the data suggest that an increase in mirror length of a factor of 3 would uniformly illuminate the module with augmented irradiance.

From 10 AM to 3 PM, nonuniformity caused by mirror augmentation occurs at a corner of module adjacent to the mirror. This nonuniformity is due to the modeled length of the mirror being equal to the length of the module, causing a nonaugmented shadow in the corner closest to the sun, unless the solar position is at its zenith. This edge effect was observed throughout the day except at solar noon when the sun is azimuthally aligned with the MAPV system. We simulated the same irradiance conditions using a mirror of length $3\times$ the module length to verify that the edge effects were related to the shortness of the mirror, as shown in Fig. 4. Furthermore, it is observed that the irradiance maps are symmetric about noon from 10 AM to 3 PM because of the similar elevation angles of the sun.

As evidenced by the 2-D irradiance uniformity plots of Fig. 3, the peak irradiance augmentation reaches nearly 1600 W/m^2 in a band that matches one complete substring; one-third of the module has uniform high irradiance, while the other two-thirds have uniformity at reduced irradiance. Because of the series connection of the cells in a module, the cells must be current

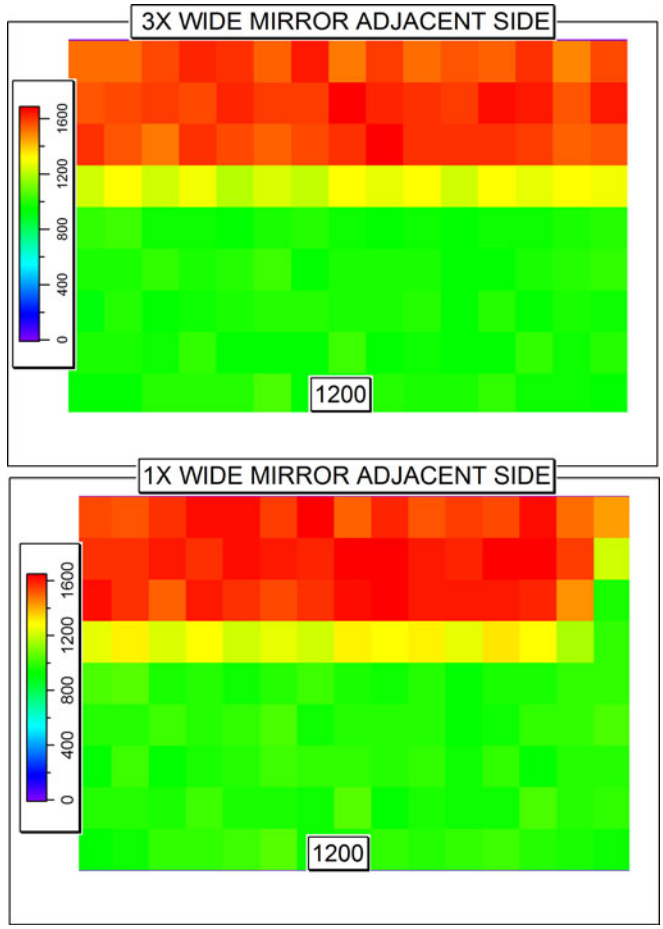

Fig. 4. Edge effects in the irradiance uniformity distribution are eliminated with a mirror that is $3\times$ longer than the module. This proof-of-concept model was not constructed but suggests that the MAPV modules at the ends of the row should be coupled with mirrors that protrude from the length of the module.

matched. That is, the smallest photoinduced current from any cell will determine the string current, and the excess photoinduced current of the high-insolation cells is lost as heat. The current matching precludes the harvesting of all incident power because the module is current limited by the least augmented region. High insolation at high nonuniformity is thus to be avoided because of potential damage from hot spots on cells. This module manufacturer's of silicon modules will subset the module into three substrings with bypass diodes in parallel with the substrings, which become forward biased when there is a current discrepancy between substrings.

In addition to the flat mirror, concave mirrors and convex mirrors were modeled. The preliminary hypothesis was that convex mirrors would distribute the reflected light over a cylindrical area. This distribution would cause less light to intercept the module, but may uniformly illuminate the module area so that the risk of forward biasing a bypass diode is reduced and thus provide more power. A corollary to that hypothesis is that the concave mirror should focus the light and greatly enhance nonuniformity. The module and mirror tilt angles are 55° and 0°, respectively, for nonflat mirrors, where the mirror tilt angle is defined as the angle to horizontal of a line tangent

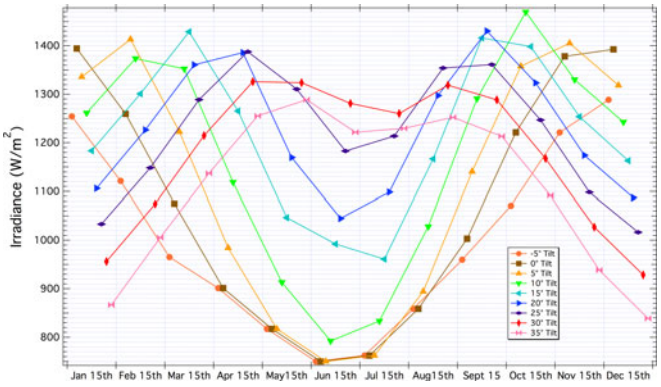

Fig. 5. Simulated peak irradiance upon a module on the 15th day of each month across a calendar year as a function of mirror tilt. The module tilt angle was fixed at 55°, where the optimum value was determined by the 1-D modeling. The curves indicate a "gullwing" shape, where the irradiance is minimum during the summer months.

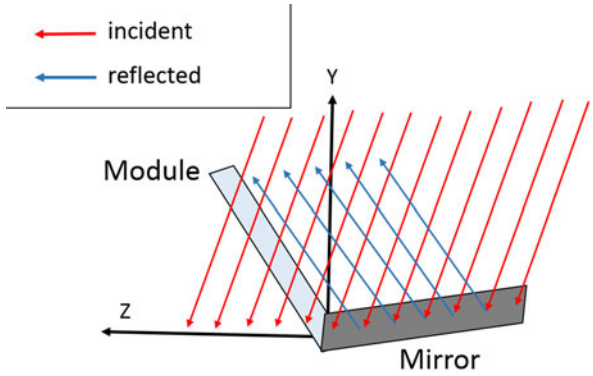

Fig. 6. Explanation of the gullwing shape is provided by TracePro simulation is shown here. Specular reflection rays from the mirror during the summer months of high solar elevation angle do not intercept the PV module at all. This sketch of a TracePro model is taken from June 15 and shows a small subset of incident light rays in red and reflected rays in blue.

to the mirror where it meets the module. TracePro confirmed these hypotheses for mirrors with various radii of curvature. For example, a concave mirror of radius of curvature equal to 250 cm increased irradiance up to 40 000 W/m^2 upon a band in the augmented region, which is not useful for an MAPV system. This nonuniformity cannot be solved even if we increase the radius of curvature to 2250 cm (nearly flat). Convex mirrors were found to be too close to the module and did not aid in uniformity unless the radius of curvature again approached infinity or flat mirrors. Hence, for uniformity and performance reasons, the flat mirror was selected for further study.

We investigated the effects of mirror tilt angle irradiance uniformity through a series of simulations to observe the irradiance distribution and determine the average irradiance by using TracePro. In these simulations, the module tilt angle was fixed at 55°, and the solar elevation and azimuth angles of noon on the 15th day of each month were selected as monthly representative samples to observe the irradiance distribution.

The 15th day of each month was picked to represent the typical power output of the month and provide a yearly variation; Fig. 5 is a plot of the peak irradiance of that day upon a MAPV module tilted 55° as a function of mirror tilt angle from −5° to 35° in steps of 5°. The results shown in Fig. 5 show a gullwing curve, i.e., the shape of the curve tends toward low values in the middle, during the summer months. This shape can be explained by studying the data and exploring the ray-tracing model output. During times of high solar elevation angles, the incident rays specularly reflected from the mirror do not intersect the module because of its tilt angle. Fig. 6 shows the ray-tracing model during summer months and depicts the reflected rays from the mirror missing the MAPV module, essentially leading to nonaugmented performance during the summer months. The data simulated for various mirror tilt angles indicate that the gullwing shape can be mitigated by tuning the mirror angles throughout different parts of the year so that the typical monthly output can be kept near maximum values. However, for cost-effective installations that require a fixed MAPV system, Fig. 7 shows the sum of the peak irradiances on the 15th day of each month versus mirror tilt angle, showing that the optimum mirror tilt angle is equal to 20° for maximum annual power production.

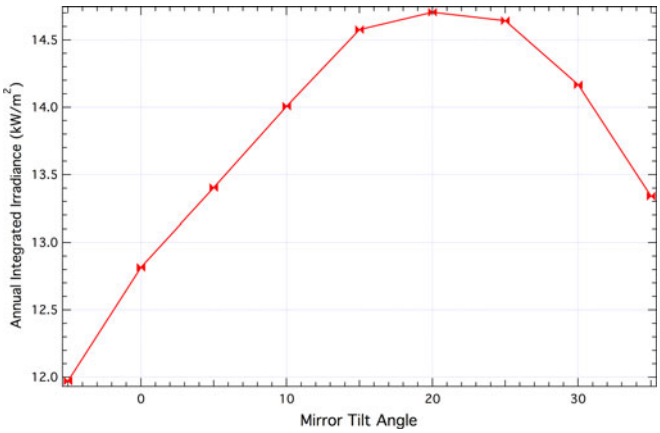

Fig. 7. Plot of the integrated results of Fig 5, showing the total annual irradiance as a function of mirror tilt for a module at 55°. The optimum mirror tilt angle for maximum annual production is 20°, even considering the significant "gullwing" shape of the time-dependent curve, as shown in Fig 5.

C. Results From Field-Testing

Fig. 8 includes three tiles plotting the measured *I–V* and *P–V* curves of a mirror-augmented and nonaugmented module, as well as the corresponding simulated PV module irradiance profile. The modules are mounted at 55°, and the mirror mounted at 0°. The maximum power output on the fixed MAPV panel is 224 W compared with 199 W of the nonaugmented panel. Although the mirror augmented I_{sc} is about 45% greater than the nonaugmented panel, the maximum power point is only 13% greater due to large irradiance nonuniformity, as evidenced by the bypass diodes becoming forward biased during the *I–V* sweep. The bottom tile of Fig. 8 shows three distinct irradiance bands upon the module: high augmentation near the mirror, moderate augmentation in the middle of the module, and low augmentation on the far edge from the mirror. These bands align well with the substring routing of a typical 60-cell module and

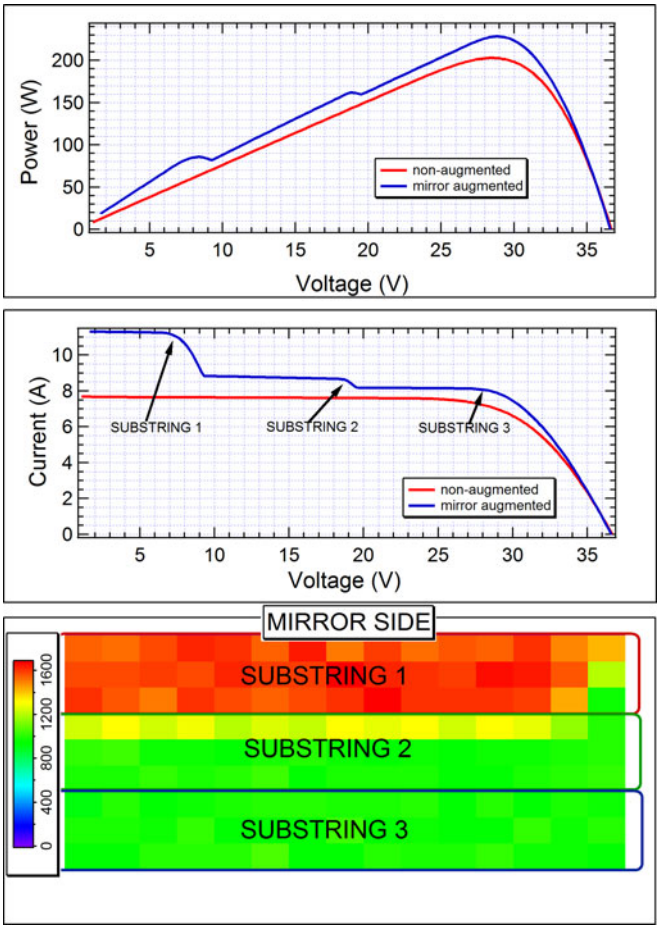

Fig. 8. Comparisons between MAPV and non-MAPV from ray-trace result and field-test site.

TABLE I
TABLE OF VALUES TAKEN FROM FIG. 8

Substring	Irradiance (W/m^2)	Predicted I_{sc} (A)	Measured I_{sc} (A)
1	1550 (120)	12.4	11.3
2	1070 (130)	8.6	9.0
3	980 (30)	7.9	8.3

The irradiance shown is the mean value from the simulation over the substring listed with the standard deviation of irradiance in parentheses. The predicted I_{sc} is calculated from the I_{sc} of the nonaugmented module and the measured POA irradiance upon the nonaugmented module. The measured I_{sc} is the y-intercept taken from a linear fit to the substring's relative low-voltage range in the I–V curve.

account for the two bypass diodes become forward biased for the two substrings nonadjacent to the mirror. The estimated irradiance in the plane of array (POA) for the nonaugmented module is 950 W/m^2, which we assume is uniform over the module, and yields a short-circuit current of 7.67 A. Table I shows the average irradiance value and standard deviation taken from the simulation over each substring area. From these irradiances and the estimated plane of array irradiance of 950 W/m^2, we estimated the model prediction of I_{sc} given the measured I_{sc} of the nonaugmented module. The results are in good agreement with the relative error among the substrings +10% (overprediction) for the

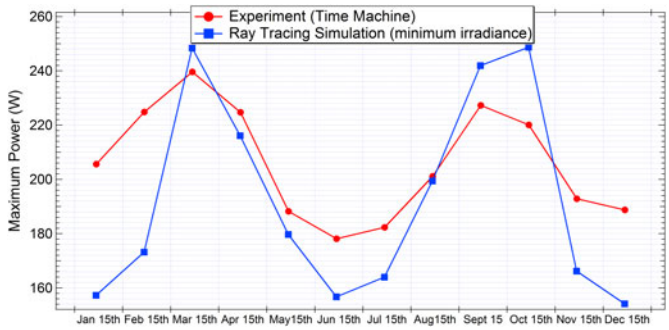

Fig. 9. Time machine measurements of maximum power point of a 200-W 60-cell pc-Si module confirms the gullwing shape of the simulation output for a module at 55° and mirror at 0°.

highest augmented substring and about −5% (underprediction) for the other two substrings. We attribute the overprediction to the high deviation, as well as observed increased shunt losses in the augmented curve compared with the nonaugmented curve. These data suggest that the ray-tracing analysis is accurate at a specific point in time and demonstrate the potential to significantly enhance the instantaneous power produced by mirror augmentation.

In addition to the I–V snapshot, power production data were recorded for a three-month period from January 6th to March 31 to demonstrate the model accuracy and power production enhancement over a longer period of time. Over this time-limited period of study, the MAPV system produced 8% more power than an equivalent nonaugmented module tilt at 55° and boosted 10% more power than the module tilt at 35°.

Computer ray tracing and the outdoor time machine measurements were used to estimate the yearly power production. The angle of the time machine was set to closely approximate the 15th day during a sunny day with high insolation, and the maximum power point of the MAPV module was recorded. The experimentally determined curve also showed a minimum during the simulated summertime, which is consistent with the gullwing shape. Fig. 9 shows the collected data from the time machine with the MAPV system and comparison with simulated results for the minimum MAPV irradiance calculated for mirror mounted at 0°. The minimum irradiance was selected for a direct comparison with the experimental data based upon the assumption that the minimum current generated in a cell determines the string current.

IV. DISCUSSION

The shape of the gullwing curve that is predicted by ray-tracing simulation using TracePro is a good match to the experimentally determined curve using the time machine. However, note that the summertime minimum is related to the observation that the mirror is not augmenting the module during high solar zenith angles, as indicated in Fig. 6, but the predicted curve is significantly below the nameplate power of 200 W, which was provided by the manufacturer at standard test conditions. This difference is caused by the optical losses from the module pitched at nonoptimal tilt angle during the nonaugmented

summer months, including increased reflectance and decreased vector component of the direct irradiance.

Because the optimal annual production for a mirror and module combination set the module at tilt angle of 55°, whereas typically a nonaugmented system would be placed a tilt angle equal to the latitude or less. Estimates of performance with two tilt angles 55° and 40°, which is the latitude in Columbus, OH, indicate an expected maximum power loss of 13% during the month of June into a module outputting. These factors would reduce the expected nonaugmented output to approximately 169 W, which is less than the experimental value and greater than the simulated prediction. Further, examination of the values shown in Table I also indicate that the average irradiance value even for a nonaugmented substring of the module tends to underpredict the measured value by approximately 5%, which ultimately accounts for the low-predicted values during the summer months. However, the experimental minimum value is about 10 W greater than the estimated nonaugmented value at 55°. These measurements indicate that there is some augmentation of the module due to the nonspecular component of light reflected from the mirror. These data also indicate the sensitivity of the results to irradiance and indicate that the ascribing a module current to the minimum cellular irradiance may not accurately model a real PV module and that the mean value over the substring area is a better measure for predictive quality.

The simulations predict higher gullwing curve peaks in Spring and Autumn than the measured values in the time machine, which may be attributed to scatter from high cloud cover that increases the relative amount of diffuse light even if the pyranometer is recording global horizontal irradiance. Thus, the clear-sky approximation of the simulations may not be adequate; however, the results are informative.

As we can see in Fig. 5, it is possible with a monthly rotation of the tilt angle of the system to eliminate the gullwing shape and have a near constant augmentation throughout the year if the effects of cloud cover are neglected. This system would require a single-axis tracker that adjusts tilt angle on a monthly timescale and would be simpler than many tracker designs for CPV. Longer mirrors would reduce the irradiance nonuniformity during the gullwing peaks during Spring and Autumn but still have no effect in summertime, effectively increasing the amplitude of the annual gullwing at the expense of the MAPV packing density.

It is difficult to estimate the effects of cloud cover and weather on the system performance. Clearly, cloudy and low-light conditions have an adverse effect on power output, but relative to the augmentation, it is not clear what other role the weather might play. In northern climates, winters tend to have low insolation, but the prevailing cloud cover is uniform and allows a modest amount of diffuse light to impact the Earth's surface. The diffuse light would not be expected to be reflected and augment the irradiance upon the module. However, the 55° tilt angle is advantageous during the winter months due to the low solar zenith over the typical latitude tilt angle, and a calculation using PVWatts indicated that this increase in power is about 4% in December.

It is also hypothetically detrimental to the lifetime performance of the module to have a high irradiance of 1600 W/m^2 incident upon the module for long periods of time or have high degrees of irradiance nonuniformity on the module. One expects that the nonuniformity causes hotspots and that the increased irradiance speeds the photolytic degradation of encapsulant materials in the module. However, the mirrors are constructed as back surface reflectors on acrylic, which absorbs the UV portion of the spectrum and does not reflect it upon the module. Therefore, the damage-inducing region of the spectrum is not augmented, and next-generation substring microconverters will be able to convert power and track maximum power for each substring at very high efficiency minimizing nonuniformity losses and hotspots.

Ultimately, the increased current may have an adverse effect on lifetime performance of the module and these experiments are underway. Recently, Peshek *et al.* [22] analyzed nine months of data collected on mirror-augmented modules mounted on two-axis trackers and characterized by complete *I–V* curves collected at 10 min intervals during that time period. During this period, no degradation in a measure of the series resistance was found for one module, and no detectable loss in fill factor was found within uncertainty. These studies persist and the analytics are ongoing.

V. Conclusion

We described a potential MAPV system that takes advantage of low pc-Si module costs and the BOS cost enhancements of a CPV system. In this study, an optimized design configuration is used to analyze the performance of a fixed (nontracked) MAPV system. Our simulations showed the nonuniformities in irradiance that arise from these mirrors and found optimal tilt angles for annual power production of 55° for the module and 20° for the coupled mirror. These simulations were compared with field-collected performance data on an MAPV system and nonaugmented module at the same site in Columbus, OH, USA. The optical analysis and experimental *I–V* data both show that the MAPV system has higher power output compared with a nonaugmented PV system. The experimental illumination patterns match ray-trace predictions well and validate the optical accuracy of our model. However, the power production from field-test is lower than predicted by the simulated results due to the nonuniformity of irradiance and forward biasing of the bypass diodes. The first prototype of fixed MAPV shows 12% boost over standard PV. Furthermore, a "gullwing" curve was found in the estimated power of fixed MAPV system over the course of a calendar year due to the large change in solar elevation angle. The irradiance uniformity and power output were affected by mirror tilt angle, and therefore, with the addition of a single-axis tracker to adjust mirror tilt throughout the year, the uniformity and power output in summer can be greatly enhanced, reducing the power variation of the gullwing curve. Additionally, power conditioning using a substring dc/dc microconverter can be installed in lieu of bypass diodes to enhance the power output of the module and more closely approach of the simulated results. These results have been simplified to exclude the effects of weather, which can have strong impact on performance, particularly on regions, such as Columbus, OH, that are in northern climates. For these climates where the winter insolation may be less than half of the peak summer insolation,

fixed MAPV systems may provide great benefit to flattening the energy harvest of PVs.

ACKNOWLEDGMENT

This work was performed at the Solar Durability and Lifetime Extension Center at Case Western Reserve University. The authors would like to thank the contributions of the research members at the VUV-Lab and Replex Plastics for their work.

REFERENCES

[1] W.-C. Lin, D. Hollingshead, R. French, K. Shell, M. Schuetz, and J. Karas, "Non-tracked mirror-augmented photovoltaic design and performance," in *Proc. IEEE 38th Photovoltaic Spec. Conf.*, Jun. 2012, pp. 002 076–002 081.

[2] M. A. Schuetz, K. A. Shell, S. A. Brown, G. S. Reinbolt, R. H. French, and R. J. Davis, "Design and construction of a 7X low-concentration photovoltaic system based on compound parabolic concentrators," *IEEE J. Photovoltaics*, vol. 2, no. 3, pp. 382–386, Jul. 2012.

[3] R. French, M. Murray, W.-C. Lin, K. Shell, S. Brown, M. Schuetz, and R. Davis, "Solar radiation durability of materials components and systems for low concentration photovoltaic systems," in *Proc. IEEE Energytech*, May 2011, pp. 1–5.

[4] B. Fortunato, M. Torresi, and A. Deramo. (2014, Apr.). Modeling, performance analysis and economic feasibility of a mirror-augmented photovoltaic system. *Energy Convers. Manage.* [Online]. vol. 80, pp. 276–286. Available: http://www.sciencedirect.com/science/article/pii/S0196890414000612

[5] P. Yadav, B. Tripathi, K. Pandey, and M. Kumar. (2014, Oct.). Effect of varying concentration and temperature on steady and dynamic parameters of low concentration photovoltaic energy system. *Int. J. Electr. Power Energy Syst.* [Online]. vol. 61, pp. 101–110. Available: http://www.sciencedirect.com/science/article/pii/S0142061514001185

[6] R. H. French, J. M. Rodriguez-Parada, M. K. Yang, R. A. Derryberry, and N. T. Pfeiffenberger, "Optical properties of polymeric materials for concentrator photovoltaic systems," *Solar Energy Mater. Solar Cells*, vol. 95, no. 8, pp. 2077–2086, Aug. 2011.

[7] M. P. Murray, D. Gordon, S. A. Brown, W.-C. Lin, K. A. Shell, M. A. Schuetz, S. Fowler, J. Elman, and R. H. French. (2011, Sep.). Solar radiation durability framework applied to acrylic solar mirrors. *Proc. SPIE, Reliab. Photovoltaic Cells, Modules, Compon. Syst. IV* [Online]. vol. 8112, pp. 811 203–811 203. Available: http://dx.doi.org/10.1117/12.893827

[8] M. P. Murray, L. S. Bruckman, and R. H. French. (2012, Nov.). Photodegradation in a stress and response framework: Poly(methyl methacrylate) for solar mirrors and lens. *J. Photon. Energy* [Online]. vol. 2, no. 1, pp. 022 004–022 004. Available: http://dx.doi.org/10.1117/1.JPE.2.022004

[9] C.-Y. Lee, P.-C. Chou, C.-M. Chiang, and C.-F. Lin. (2009). Sun tracking systems: A review. *Sensors* [Online]. vol. 9, no. 5, pp. 3875–3890. Available: http://www.mdpi.com/1424-8220/9/5/3875/pdf

[10] M. Rivera, G. C. Roach, J. N. Mitchell, and J. L. Boehme. (2013, May). System-level solar module optimization. *Proc. SPIE, Energy Harvesting Storage, Mater., Devices, Appl.* [Online]. *8728*, pp. 87 280Q-1–87 280Q-12. Available: http://dx.doi.org/10.1117/12.2016141

[11] C. Deline, J. Meydbray, M. Donovan, and J. Forrest. (2012). Photovoltaic shading testbed for module-level power electronics. *Contract* [Online]. *303*, pp. 275–300. Available: http://enphase.com/global/files/NREL-Study-on-Shading.pdf

[12] C. Olalla, C. Deline, and D. Maksimovic, "Performance of mismatched PV systems with submodule integrated converters," *IEEE J. Photovoltaics*, vol. 4, no. 1, pp. 396–404, Jan. 2014.

[13] I. Reda and A. Andreas. (2003). *Solar position algorithm for solar radiation applications*. [Online]. Nat. Renewable Energy Lab. Golden, CO, USA. Available: http://oretano.iele-ab.-uclm.es/∼carrion/Bibliografia/Solar%20Position%20Algorithm%20for%20Solar%20Radiation%20Applications.pdf

[14] F. Kasten and A. T. Young. (1989, Nov.). Revised optical air mass tables and approximation formula. *Appl. Opt.* [Online]. vol. 28, no. 22, pp. 4735–4738. Available: http://ao.osa.org/abstract.cfm?URI=ao-28-22-4735

[15] A. B. Meinel and M. P. Meinel. (1977). Applied solar energy: An introduction. *NASA STI/Recon Technical Report A* [Online]. vol. 77, p. 33445. Available: http://adsabs.harvard.edu/abs/1977STIA...7733445M

[16] A. Terao, O. Chao Pujol, S. G. Daroczi, N. R. Kaminar, D. D. Smith, R. M. Swanson, P. Benitez, J. L. Alvarez, and J. C. Minano. (2002). Recent developments on the flat-plate micro-concentrator module. *Proc. IEEE 29th Conf. Rec. Photovoltaic Spec. Conf.*[Online]. pp. 1373–1376. Available: http://ieeexplore.ieee.org/xpls/abs_all.jsp?arnumber=1190864

[17] W.-C. Fei, C.-H. Huang, W.-C. Hsu, and J.-C. Tsai, "Design and simulation of a secondary solar concentrator constructed with a circular micro prism array for the enhancement of the concentration ratio," in *Proc. IEEE 34th Photovoltaic Spec. Conf.*, Jun. 2009, pp. 001 727–001 731.

[18] H.-Y. Pan, S.-H. Chang, B.-H. Ke, and K.-J. Chen, "The study on the allowing angle of the sun's rays of concentrated photovoltaic (CPV) concentrator," in *Proc. Int. Conf. Elect. Control Eng.*, Sep. 2011, pp. 6185–6188.

[19] Y. Ota and K. Nishioka. (2011). Tracking error analysis of concentrator photovoltaic module using total 3-dimensional simulator. *Proc. 7th Int. Conf. Concentrating Photovoltaic Syst.* [Online]. vol. 1407, pp. 281–284. Available: http://scitation.aip.org/content/aip/proceeding/aipcp/10.1063/1.3658344

[20] Y. Ota, Y. Sakurada, and K. Nishioka. (2012, Jul.). 2-dimensional mapping of power consumption due to electrode resistance using simulator for concentrator photovoltaic module. *Mater. Sci. Forum* [Online]. vol. 725, pp. 183–186. Available: http://www.scientific.net/MSF.725.183

[21] Y. Ota and K. Nishioka. (2012, Jan.). Three-dimensional simulating of concentrator photovoltaic modules using ray trace and equivalent circuit simulators. *Solar Energy* [Online]. vol. 86, no. 1, pp. 476–481. Available: http://www.sciencedirect.com/science/article/pii/S0038092X11003884

[22] T. J. Peshek, S. Mathews, Y. Hu, and R. H. French, "Mirror augmented photovoltaics and time series analytics of the I–V curve parameters," in *Proc. IEEE 40th Photovoltaic Spec. Conf.*, Jun. 2014, pp. 2027–2031.

Wei-Chun Lin (S'12) is currently working toward the Ph.D. degree with Case Western Reserve University, Cleveland, OH, USA.

His previous working experience focused on surface analysis of organic materials with Academia Sinica, Taiwan. His current research interests include clean energy devices and its characterization.

Timothy J. Peshek (M'14) received the Ph.D. degree in physics from Case Western Reserve University, Cleveland, OH, USA, in 2008, in research devoted to the thermodynamics of growth of GaN and vibrational spectra of $ZnGeN_2$.

He is a Research Assistant Professor of materials science and engineering, Case Western Reserve University, with an adjunct appointment with the Department of Physics. Prior to this appointment, he was working as a Team Leader in design and reliability of a novel microinverter concept with a startup called *e*QED, LLC, Mayfield Village, OH, for three years following a Postdoctoral Scholar appointment at Arizona State University, Tempe, AZ, USA, in-residence with the National Renewable Energy Laboratory in Golden, CO, USA, developing thin-film polycrystalline solar cells based upon novel, earth-abundant II–IV–V compound semiconductors.

Laura S. Bruckman received the Ph.D. degree in analytical chemistry from the University of South Carolina, Columbia, SC, USA, in August 2011.

She is a Research Associate with Case Western Reserve University (CWRU), Cleveland, OH, USA. Her research interests with the University of South Carolina include developing methods for the rapid classification of phytoplankton cells using single-cell fluorescence measurements, optical trapping, and multivariate optical computing. Her research with CWRU has been focused on the degradation mechanisms of acrylic and acrylic back surface mirrors to apply the stress and response framework in lifetime and degradation science. Her research experiences bring together statistical analytics with big data type problems.

Mark A. Schuetz (M'11) received the Bachelor of Science degree in mechanical engineering and the Master of Science degree from the Massachusetts Institute of Technology, Cambridge, MA, USA.

He is the Founder and President of Replex Plastics, Mount Vernon, OH, USA. Founded in 1991, Replex Plastics has become a world leader in the manufacture of convex acrylic mirrors, polycarbonate playground domes, and thermoformed closed-circuit TV domes.

Roger H. French (M'08) received the B.S. degree from Cornell University, Ithaca, NY, USA, and the Ph.D. degree in materials science from the Massachusetts Institute of Technology, Cambridge, MA, USA.

He has been the F. Alex Nason Professor with the Department of Materials Science and Engineering, Case School of Engineering, with secondary appointments in macromolecular science and physics at Case Western Reserve University, Cleveland, OH, USA, since August 2010. He is the Director of the Solar-Durability and Lifetime Extension center, which focuses on lifetime and degradation science of long-lifetime environmentally exposed materials, components, and systems such as solar energy technologies, energy-efficient lighting, roofing, building exteriors, etc. Before this, he was with Central Research and Development, DuPont Co., Wilmington, DE, USA, beginning in 1985 and was an Adjunct Professor of materials science with the University of Pennsylvania, PA, USA, beginning in 1996. Using vacuum ultraviolet and optical spectroscopies, spectroscopic ellipsometry, and computational optics, his research interests include optical properties, electronic structure, and radiation durability of optical materials, polymers, ceramics, and liquids. He has published 22 issued patents and more than 145 publications.